Nanomed Res J 6(3):237-247, Summer 2021

RESEARCH ARTICLE

A polysaccharide of Ziziphus spina-Christi L., and it's Silver nanoparticles induced reactive oxygen species and late apoptosis in Liver cancer cells

Haneen K. Thawini[1,2], Ali A. A. Al-Shawi[1*]

[1] *Chemistry Department, College of Education for Pure Sciences, University of Basrah, Basrah, Iraq*

[2] *Chemistry Department, College of Education/Qurnah, University of Basrah, Basrah, Iraq*

ARTICLE INFO

Article History:
Received 19 May 2021
Accepted 14 Jul 2021
Published 01 Aug 2021

Keywords:
Biopolymers
Zizphus spina-christi species
Polysaccharides
Polysaccharide coated AgNPs
Flow cytometry analysis

ABSTRACT

Objective(s): Ziziphus spina-Christi is a Ziziphus genus, and its extracts have been tested for antimicrobial, antifungal, and antitumor properties. A polysaccharide and its silver nanoparticle from the Ziziphus spina-Christi plant have not yet been tested for their ability to fight liver cancer.

Methods: Using a microwave-assisted extraction method, we extracted polysaccharide from the leaves and synthesized silver nanoparticles. The polysaccharide amount, availability, and nanoparticle properties were investigated using the phenol-sulfuric acid process, FT-IR, SEM, TEM, and XRD. The anticancer activity of crude polysaccharide and its polysaccharide coated AgNPs were investigated using the HepG2 cancer cells, MTT assay, cell morphology, cell cycle, reactive oxygen species (ROS), and apoptosis.

Results: The existence of predominantly spherical shapes and various sizes (24.10, 29.77, 31.63, 47.7, 56, and 71.5) nm polysaccharide coated AgNPs was confirmed by SEM and TEM analysis. Using the Debye-Scherrer formula, XRD analysis revealed six peaks corresponding to the crystalline size (D value) of AgNPs. Polysaccharide-coated AgNPs outperformed raw polysaccharide against HepG2 cancer cells. Polysaccharide had an IC50 of 1.5 mg/ml in the MTT assay, while polysaccharide coated AgNPs had an IC50 of 0.705 mg/ml. According to a flow cytometry study, raw polysaccharide stopped cells in the S process, but polysaccharide coated AgNPs arrested cells in the G1 phase. Furthermore, raw polysaccharide late apoptosis was lower than late apoptosis of nanoparticles induced by reactive oxygen species.

Conclusions: The findings indicated that polysaccharide coated AgNPs derived from Ziziphus spina-Christi polysaccharide could be developed as an anticancer agent against liver cancer and that further research for potential applications is warranted.

How to cite this article
Thawini H.K., Al-Shawi A.A.A. A polysaccharide of Ziziphus spina-christi L., and it's Silver nanoparticles induced reactive oxygen species and late apoptosis of Liver cancer cells . Nanomed Res J, 2021; 6(3): 237-247. DOI: 10.22034/nmrj.2021.03.0004

INTRODUCTION

Natural medicinal plant products have a lot of potential in medical applications because they contain small and large molecules from primary and secondary metabolism **[1,2]**. Natural product compositions and chemical structures are essential in the production of biological activities **[3,4]**. Biopolymer is a natural product that is produced during the life cycles of green plants, animals, bacteria, and fungi and has a variety of biological functions **[5,6]**. Furthermore, animal biopolymers such as gelatin, collagen, and carbohydrates are used in the food industry and biomedical science **[7]**. Polysaccharide, a biopolymer that includes linear and branched polymeric carbohydrates including lignin, cellulose, cutin, and cutan, is produced by plants **[8]**. Polysaccharides are used

* Corresponding Author Email: *ali.abdulhussein@uobasrah.edu.iq*

in a variety of biological applications, including medication formulations, dusting powder, treatment of mild intestinal disorders, hemostats, plasma replacement, and anticoaguables [**9,10**]. Antitumor properties have been identified in polysaccharides isolated from plants, fungi, marine sources, and microorganisms [**11,12**]. As a result, some studies have suggested that polysaccharides may have anti-liver properties [**13**].

Ziziphus is a Rhamnaceae (Buckthorn) genus with about 40 species. *Ziziphus jujuba* grows in Southern Asia, Northern India, Southern and Central China, and Southeastern Europe. The polysaccharides isolated from *Zizphus jujuba* have a variety of biological applications, according to the findings [**14**]. Similarly, the development of Ziziphus spina-Christi in Northern and Tropical Africa, Southern and Western Asia, and the Middle East is known as (Sidr) [**15**]. *Ziziphus* leave extracts have been shown in recent studies to be effective in reducing extreme inflammation [**16**]. There have been no reports of isolated/extract polysaccharides from *Ziziphus spina-Christi* species of leaves. Nanoparticles are also used in biological applications because of their ability to penetrate cell membranes or drug carriers, and they are a promising cancer treatment choice [**17**]. To generate four unique nanosystems, metallic nanoparticles (Ag), bimetallic or alloy nanoparticles (Fe-Co), metal oxide nanoparticles (ZnO), and magnetic nanoparticles (Mn–Fe2O4) are used. These metals will find new applications in drug delivery, cancer therapy, bio-imaging magnetic hyperthermia, photoablation therapy, and biosensors in nanopaticle systems. Because of their stable features such as high electrical conductivity, high thermal conductivity, chemical stability, catalytic activity, and improved Raman scattering, silver nanoparticles are used in drug delivery and cancer therapy applications [**18**]. Silver nanoparticles perform critical roles in cancer cells, such as functional heterogeneity, microenvironmental variations, and reversible alterations in cell characteristics. These functions heighten interest in synthesizing various silver nanoparticles from natural sources [**19**]. Many studies have synthesized silver nanoparticles from medicinal plant aqueous extracts and tested them in a variety of medicinal applications [**20,21**]. In addition, nanoparticles of polysaccharides from medicinal plants such as Chitosan and Arabinoxylan, have been synthesized and their biological properties investigated [**22,23**]. As a result, nanoparticles have been used in hepatocellular disease research as therapeutics and diagnostics, but more research into nanoparticles as therapeutic agents is still required [**24,25**]. As a result, this research used a microwave-assisted extraction green method to extract polysaccharides from leaves, synthesize silver nanoparticles, and investigate anticancer properties using the HepG2 cancer cells, MTT assay, cell cycle, reactive oxygen species, and apoptosis.

MATERIALS AND METHODS

Plant collection

The leaves of *Ziziphus spina-Christi* (L.) were collected from a garden in the Al-Medina district of Basra Governorate, Southern Iraq, during September 2019, and identified by Prof. Dr. Ali Aboud, Department of Life Sciences - College of Education for Pure Sciences - Basrah University. The leaves were dust-free, washed in distilled water, and dried for a week in the shade. Milled and stored in closed, opaque glass containers in the refrigerator at 4 degrees Celsius until required.

An FT-IR Shimadzu device with KBr discs with a range of (400-4000) cm-1 at room temperature was utilized in the Department of Chemistry, College of Education for Pure Sciences, University of Basrah.

Method for extracting polysaccharides from the Ziziphus spina-Christi plant

In a round flask, weigh 10 gm of dried *Ziziphus spina-Christi* (L.), add 100 ml of ionized water, mix well, and microwave for 30 minutes. To remove sediments, the microwave is turned on for (60-120) seconds, cooled for 15 minutes, and centrifuged (5000 rpm for 15 minutes). The residual sediments were filtered under vacuum pressure to remove them. The filtrate was placed in a beaker, and the volume of absolute ethanol (96 percent) was slowly added three times in the beaker with constant stirring, and the solution was held in the refrigerator at 4 °C for 24 hours. The precipitated was collected and centrifuged (5000 rpm for 20 minutes). The filtrate is extracted, and 1 ml of water is added to the tube to absorb the precipitate. Re-sedimentation in the centrifuge at the same speed to remove the remaining water and obtain the *Z. spina-Christi* crude polysaccharides (L.) [**26**].

Sevag method for deproteinatation of polysaccharides

The protein is extracted by applying a volume

(3:1) CHCl3-n-BuOH to 60 ml raw polysaccharide in a separation funnel, shaking for 10 minutes, and allowing the mixture to settle for 20 minutes (organic layer and aqueous layer). Proteins collect in the lower layer (the organic layer) and are removed from the separating funnel. The raw polysaccharides were precipitated by adding three times the amount of absolute ethanol (96%) to the aqueous layer and shaking it. Refrigerated for an hour at 4 °C before being deposited in the centrifuge (8000 rpm for 30 minutes). To obtain raw multiple polysaccharides free of protein, this process is replicated several times [**27**]. The supply of raw polysaccharide was determined using FTIR.

Quantitative of polysaccharide content (phenol-sulfuric acid method)

In a test tube, placed 100 mg of glucose and 5 ml of 2.5 N HCl, then place it in a boiling water bath for 3 hours for glycolysis. Allow to cool to room temperature before adding a sufficient amount of sodium carbonate to bring the total volume to 100ml. 0.2, 0.4, 0.6, and 0.8 ml of the solution were taken, and 1 ml of 5 % phenol solution was applied to each sample and shook well. The absorbance was measured at 490 nm after adding 5 ml of 96 % sulfuric acid, shaking again, leaving for 10 minutes, shaking again, and placing in a water bath for 20 minutes. The linear equation was used to calculate the content of saw polysaccharide using the raw polysaccharide method with 0.1 ml solution and the absorbance at 490 nm (1) [**27**]**.**

$$y = 0.1539x + 0.7655 \quad (1)$$

Which: y = The value of absorbance at 490 nm; x= Carbohydrate concentration

$$\%Total\ carbohydrate = \frac{x}{0.1}x100 \quad (21)$$

Polysaccharide coated silver nanoparticles synthesized

1 ml raw polysaccharide was applied to 49 ml AgNO3 (1 mm), gently mixed, and held inside the microwave instrument for 20 minutes, according to Ali et al. method with some modifications [**28**]. 1 minute at 50 °C and 400 W, until the color changed to show the formation of silver nanoparticles. Cooled AgNPs at room temperature and washed twice with distilled water before centrifuging at 8000 rpm for 15 minutes, removing the water and storing the residual at 4 °C for further characterization and anticancer evaluation. SEM, EDX, TEM, and XRD techniques were used to analysis the sizes, ratio, and shapes of polysaccharide coated silver nanoparticle.

AgNPs Characterization techniques

All of the characterization methods for AgNPs analysis were carried out at Tehran University's Central Laboratory in Iran. .

Scanning electron microscope (SEM)

A modest amount of AgNPs was put on carbon-coated copper and studied with an FEI Nova Nano SEM equipped with energy-diffraction X-ray spectroscopy (EDX). The photo was captured at a magnification of 60.00 [**29**].

Transmission electron microscopy (TEM)

Philips CM30 electron microscope was used to perform an AgNPs TEM image. Deposition of a powder suspension in ethanol on carbon coated copper microgrids was used to create TEM specimens [**30**].

X-ray diffraction (XRD)

Using a Philips PW 1730 from (2θ (5-80)) using Cu, K-α , λ =1.54060, the phase transformation during the sonochemical reaction and sintering was determined. Using the Debye-Scherrer formula, the average crystalline size D of the AgNPs was determined from the diffractogram [**31**]:

$$D = \frac{0.9\,x\,\lambda}{\beta\,x\cos\theta}$$

where D is the approximate crystal size, λ is the X-ray radiation wavelength (1.54 Å), θ is the Braggs angle corresponding to the most intense peak, and β is the peak's complete width at half maximum in radians.

MTT assay

The MTT test was done on 96-well plates to determine the IC_{50} of polysaccharide and its silver nanoparticles. $1x10^4$ cells per well were planted into the HepG2 cell lines. After 24 hours of incubation, the cells were treated with different doses (0.500-2.500) mg/ml made in distilled water, using the standard dilution process to obtain five

concentrations, and their effect was evaluated for 72 hours. The growing medium was removed and replaced with 28 µL of MTT solution, which was incubated for 2 hours at 37 °C. After extracting the MTT solution, 100 µL of DMSO (Dimethyl Sulfoxide) was given to the cells, which were then incubated at 37 °C for 15 minutes. Using a micro-plate reader, the absorbance was measured at 620 nm, and the cell viability % was computed based on the concentrations **[32]**.

Flow cytometry analysis
Cell Cycle arrest

Flow cytometry analysis has defined the G1, S, and G2 phases. HepG2 cells were subjected to IC_{50} values of raw polysaccharide and AgNPs for 48 hours. The cells were rinsed in PBS before being fixed overnight in 70% ice-cold ethanol at 4 °C. Cells were stained for 30 minutes in the dark at room temperature with a solution containing 50 mg/mL PI and 100 mg/mL RNase A after being washed twice with phosphate buffer saline (PBS). The stained cells were examined using flow cytometry (manufacturer: PARTEC; model: CyFlow Space; made in : Föreningsgatan 217, 261 51 Landskrona, Germany; software: FLOWMA) **[33]**.

Reactive oxygen species

The alterations in intracellular reactive oxygen species formation were measured by labeling the cells with 2,7-dichlorfluorescein-diacetate (DCFH-DA). In 6-well culture plates, the cells were incubated overnight. Following a 48-hour treatment with the IC_{50} values of raw polysaccharide and AgNPs, the cells were incubated for 30 minutes at 37 °C with 10 mol/l DCFH-DA, as indicated by the manufacturer. The cells in the positive control group were tagged with DCFH-DA and raised for 30 minutes after being treated with 1 µL. Cells were then collected, washed, and re-suspended in phosphate buffer saline (PBS) before being flow cytometrically examined for 2,7-dichlorfluorescein (DCF) fluorescence **[34].**

Apoptosis

The late apoptosis was classified by flow cytometry. Raw polysaccharide and AgNPs IC_{50} values were applied to HepG2 cells for 48 hours. The cells were collected, washed twice with phosphate buffer saline (PBS), and tagged with 5 µL FITC-conjugated annexin V, as directed by the manufacturer. After being incubated in the dark for 10 minutes and then labeled with PI, the samples were immediately examined on a flow cytometery **[35]**.

Statistical analysis

The raw polysaccharide and AgNPs IC_{50} values were estimated using GraphPad Prism 8.1 for Windows. The experiments were carried out three times.

RESULTS AND DISCUSSION

Analysis and characterization of raw polysaccharide and it's Silver nanoparticles

Water extraction, acid-base assistance, enzymatic hydrolysis, ultrasonic and microwave-assisted extraction, and polysaccharide precipitation with alcohol are among the most popular extraction methods for plant polysaccharides. Microwave-assisted extraction, for example, is a low-cost, high-efficiency technique for plant extraction and nanoparticle synthesis **[36,37]**. In this study, silver nanoparticles of polysaccharide from *Ziziphus spina-Christi* (L.) species were extracted and synthesized using a microwave-assisted technique. It was because of the simple process, the short time frame, and the high quality of the goods (**Fig.** 1). We used FT-IR spectroscopy and the phenol-sulfuric acid process to determine the abundance of raw polysaccharide. Stretching vibration of C-OH was referred to by the broad peak 3600 to 3200 cm^{-1}. The stretching vibration of C=O and the asymmetric stretching vibration of C=O were referred to as the peak between 1500 and 1700 cm^{-1}. C-H stretching vibrations were assigned to the peaks 1250 to 1550 cm^{-1}. O-H stretching vibrations were defined as a weak peak ranging from 500 to 700 cm^{-1}. Peaks between 1000 and 1200 cm^{-1} indicated the existence of C-O-C glycosidic bonds, while a weak peak about 849 cm^{-1} indicated the presence of a glycoside bond **[32]** (**Fig.** 2 (A)). The FT-IR analysis confirmed the availability of raw *Ziziphus spina-Christi* polysaccharide.

The carbohydrate content is estimated using the phenol-sulfuric acid method and glucose as a standard. At 490 nm, a linear plot and **equation** (1) were used to estimate the carbohydrate content (**Fig.** 2 (B)). Equation (2) was used to calculate the total carbohydrate content of *Ziziphus spina-Christi*, which was 0.86 percent based on the approximate absorbance value (0.892) and 0.1 ml of raw polysaccharide. Metal nanoparticles can also be created using a variety of chemical and physical

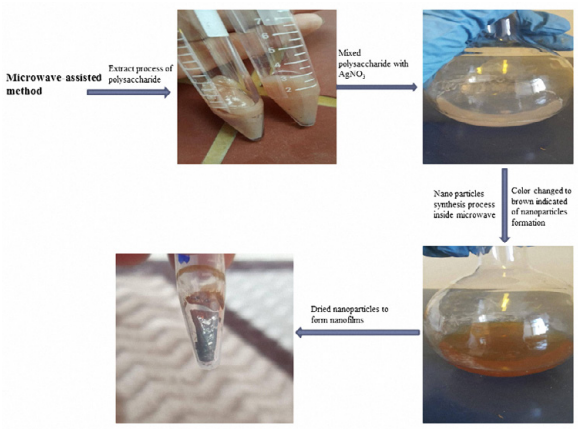

Fig. 1. Using a microwave-assisted extraction technique, the steps of extraction and synthesis of raw polysaccharide and its AgNPs were demonstrated.

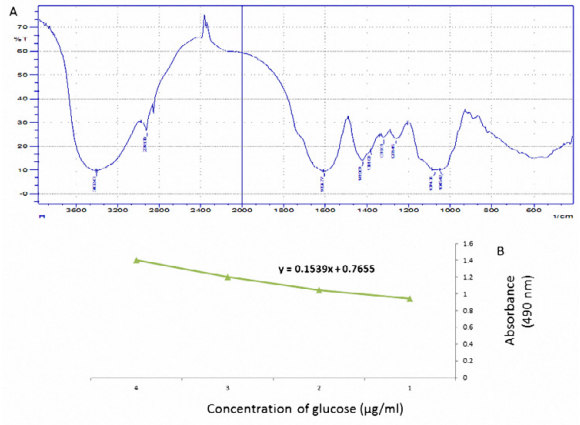

Fig. 2. A- FT-IR analysis of raw polysaccharide of *Ziziphus spina-christi.* B- Phenol-sulfuric acid method of glucose at 490 nm to estimate the content of raw polysaccharide of *Ziziphus spina-christi.*

methods, including gamma irradiation, chemical reduction photochemical, thermal decomposition, and microwave irradiation. Among these methods, microwave is a simple and quick way to create metal nanoparticles. Microwave synthesis of polysaccharide coated silver nanoparticles from *Ziziphus spina-Christi* was used in our study, the formation of nanoparticles was easily detected after 30 seconds by changing the color of the solution from translucent to brown. SEM-EDX, TEM, and XRD were used to characterize the morphology, form, and scale of nanoparticles. SEM is a soft technique used to analyze particle sizes, size distributions, shapes, and surface morphology of nanoparticles at the micro and nanoscales. The particles can be manually measured and counted using specific software based on the SEM images. SEM and energy-dispersive X-ray spectroscopy (EDX) combined can provide AgNPS morphology and chemical composition analysis. It can provide useful information about purity and aggregation of particle.

In this study, SEM image revealed that raw polysaccharide was free of silver metal and had aggregation coherent shapes, an EDX spectrum demonstrated that the polysaccharide is free of Ag metal (**Fig.** 3(A)). While SEM images of polysaccharide coated AgNPs (29.77, 31.63, and 24.10) nm in size and spherical in shape were shown, an EDX spectrum revealed a silver ratio of 16.6. Wt% (**Fig.** 3(B)).

We analyzed AgNPs using the TEM technique, which is an important technique for nanoparticle characterization. Sample preparation and time consumption are critical for obtaining the highest resolution and quality of images in TEM. It was

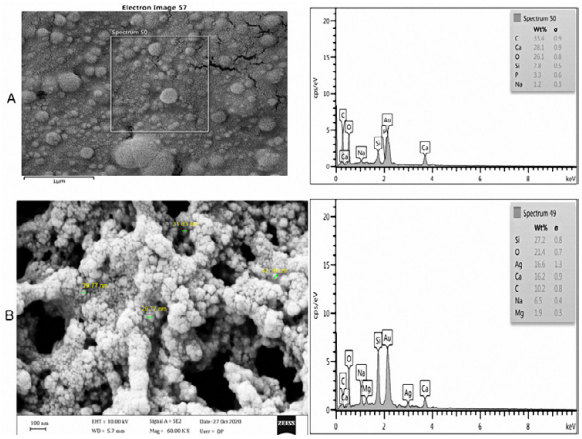

Fig. 3: SEM-EDX analysis of : A- Raw polysaccharide. B- AgNPs.

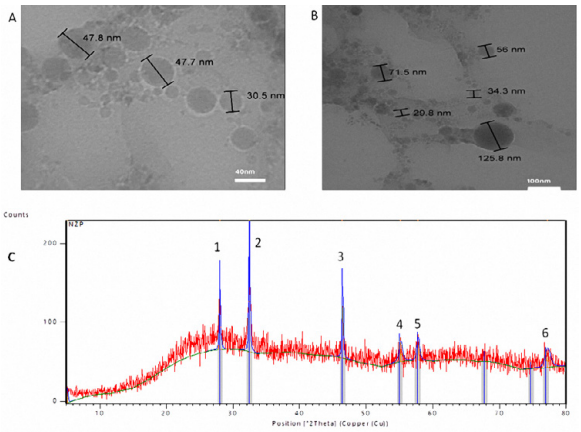

Fig. 4. Characterization of AgNPs utilizing: A- TEM analysis at 40 nm. B- TEM analysis at 100 nm. C- XRD analysis.

used to obtain quantitative particle, grain, size distribution, and morphology measurements. TEM has two advantages: higher spatial resolution and the ability to perform additional analytical measurements. In our study, TEM analysis revealed the spherical shapes of AgNPs; in image 40 nm, the spherical size of AgNPs showed (30.5, 47.7, and 47.8) nm (**Fig.** 4A), while image 100 nm revealed (29.8, 34.3, 56, 71.5, and 125.8) nm (**Fig.** 4B).

Furthermore, XRD is a technique with many applications, including molecular and crystal structure analysis, qualitative identification of various compounds, quantitative resolution of chemical species, measuring crystallinity, isomorphous substitutions, and particle sizes. The application of XRD has grown to include the characterization of various nanomaterials and their properties. We used an XRD pattern to confirm the crystallinity of polysaccharide coated AgNPs formation in our study, and we obtained six peaks. We estimated the crystalline size (D) for the six peaks (1 = 6.7 nm, 2 = 8.3 nm, 3 = 8.5 nm, 4 = 3.8 nm, 5 = 5.5 nm, and 6 = 6.6 nm) at 2 theta using the Debye-Scherrer formula (**Fig.** 4C). The six D values are nearly identical, and the average crystalline size of AgNPs is about 6 nm. D spacing also showed nearly the same value for the six peaks, with an average of 2 Å, shown in **Table** 1. These XRD data values confirm the formation of polysaccharide coated AgNPs crystallites with well-defined dimensions.

Anticancer evaluation of raw polysaccharide and it's AgNPs

Polysaccharides from different sources have been shown to disrupt cancer cells via induced apoptosis and mechanistic studies **[38,39]**. As a result, some polysaccharides, such as Ganoderma

Table 1. The XRD analysis of AgNPs was shown, and we estimated the crystalline size (D value) for six peaks (1 = 6.7 nm, 2 = 8.3 nm, 3 = 8.5 nm, 4= 3.8 nm, 5= 5.5 nm, and 6= 6.6 nm) using the Debye-Scherrer formula.

Peak No	2 θ	Cos θ	Crystalline size 'D' nm	Height [cts]	FWHM Left [°2Th.]	d-spacing [Å]	Rel. Int. [%]	Tip Width	Matched by
1	28.0298	0.882	6.7	56.59	0.2362	3.18340	44.19	0.2834	00-031-1238
2	32.4336	0.844	8.3	128.07	0.1968	2.76052	100.00	0.2362	00-031-1238
3	46.4419	0.689	8.5	73.92	0.2362	1.95531	57.72	0.2834	00-031-1238
4	55.1493	0.571	3.8	18.49	0.6298	1.66544	14.44	0.7557	00-031-1238
5	57.7645	0.533	5.5	20.83	0.4723	1.59611	16.26	0.5668	00-031-1238
6	77.1520	0.222	6.6	17.27	0.9446	1.23636	13.49	1.1336	00-031-1238

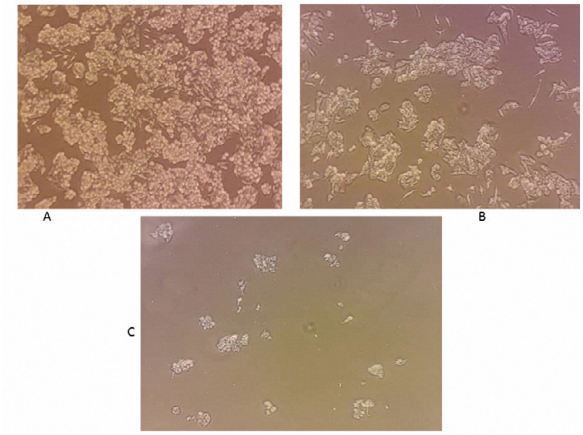

Fig. 5. Liver cancer cell morphology changes: A- Untreated cells. B- Cells treated with IC_{50} value of raw polysaccharide. C- Cells treated with IC_{50} value of AgNPs.

sinense and Ganoderma lucindum, may be used to treat cancer [**40**]. Green synthesis of polysaccharide coated silver nanoparticle has been shown to have a potential role in cancer prevention by drug delivery systems [**41,42**]. In this study, for the first time, we investigated the anticancer activity of raw polysaccharide and polysaccharide coated silver nanoparticle from the *Ziziphus spina-Christi* species against liver cancer cells (HepG2). The MTT assay was used to measure IC_{50} values, which were 1.5 mg/ml for raw polysaccharide and 0.705 mg/ml for AgNPs.

In comparison to untreated cells as a control, the morphology of cells influenced by IC_{50} values revealed that nanoparticles had a greater effect than raw polysaccharide (**Fig.** 5 (A, B, and C)). Furthermore, flow cytometry analysis was used to determine the differences in efficacy between raw polysaccharide and its AgNPs.

As compared to the control result, raw polysaccharide stopped cells in the S gate (**Fig.** 6 (A and B)), whereas AgNPs stopped cells in the G1 gate (**Fig.** 7 (A and B)). The reactive oxygen species ratio using DCFH of raw polysaccharide was 59 percent (**Fig.** 6 (C)), and for AgNPs was 31 percent (**Fig.** 7 (C)), respectively, compared to 99.7% (**Fig.** 6 and 7 (D and D)). This means that AgNPs is more efficient than raw polysaccharide in reducing reactive oxygen species. As a result of the apoptosis study, late apoptosis (Q2) of raw polysaccharide was 3.03 percent (**Fig.** 6 (E)), while late apoptosis of AgNPs was 10.9 percent (**Fig.** 7 (E)), as opposed to late apoptosis of control (Q4), (**Fig.** 6 and 7 (F and F)). The ability of AgNPs of *Ziziphus spina-Christi* polysaccharide to increase late apoptosis more effectively than raw polysaccharide demonstrated that nanoparticles of *Ziziphus spina-Christi* polysaccharide are more effective and could pave the way for further mechanistic research into apoptosis pathways.

Because of their cellular signaling abilities, ROS play a role in cancer prevention. It promotes protumorigenic signaling, allowing cancer cells to proliferate, survive, and adapt to hypoxia. Although anticancer medicines with direct ROS accumulating activity have been demonstrated to

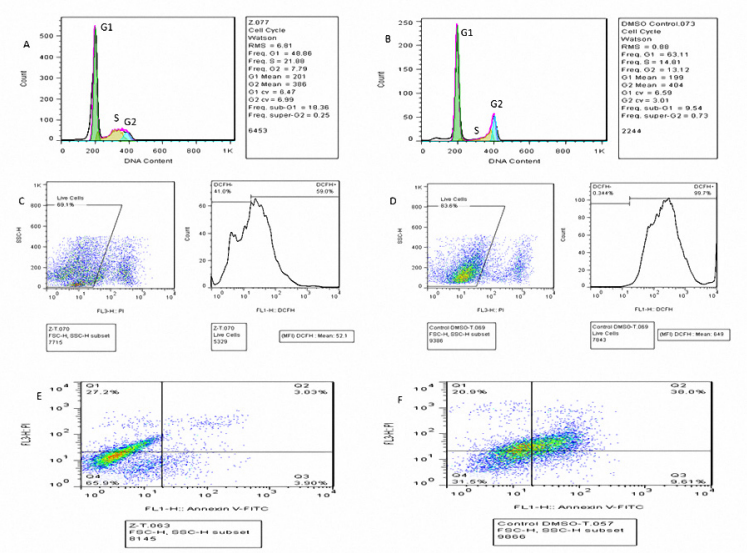

Fig. 6. Flow cytotometry analysis of raw polysaccharide: A- Cells cycle of treated cells with IC_{50} value. B- Cell cycle of untreated cells. C- Reactive oxygen species of treated cells with IC_{50} value. D- Reactive oxygen species of untreated cells. E- Apoptosis of treated cells with IC_{50} value. F- Apoptosis of untreated cells.

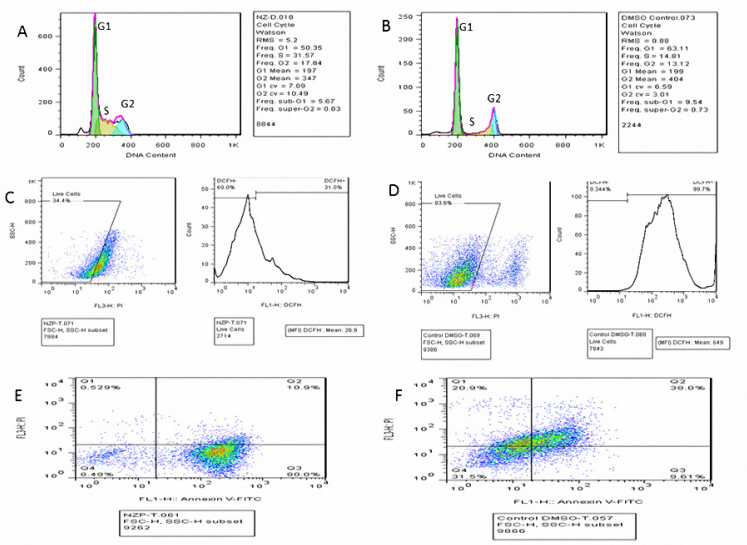

Fig. 7. Flow cytotometry analysis of AgNPs: A- Cells cycle of treated cells with IC_{50} value. B- Cell cycle of untreated cells. C- Reactive oxygen species of treated cells with IC_{50} value. D- Reactive oxygen species of untreated cells. E- Apoptosis of treated cells with IC_{50} value. F- Apoptosis of untreated cells.

be successful in treating several forms of cancer, their effects on normal cells remain controversial because they affect both cancer and normal cells [**43**]. In addition, nanotechnology provides six major categories that can be exploited in nanomedicine (carbon NPs, metal NPs, ceramic NPs, semiconductor NPs, polymeric NPs and lipid-based NPs). Metal-containing nanoparticles (NPs) enhance ROS formation via the Haber-Weiss and Fenton-type reactions. Metal nanoparticles' ability to generate ROS generation is greatly controlled by their size and form [**44**]. Metallic nanoparticles' versatility can improve drug delivery to tumor cells while decreasing toxicity. Metallic nanoparticles can be used to treat cancer at the cellular and subcellular levels, reducing side effects and greatly

improving therapeutic efficacy. Another difficulty in cancer therapy is using novel nanoparticles in single platform-based techniques to achieve higher specificity, lower toxicity, biocompatibility, safety, and efficacy while overcoming the limits of traditional chemotherapy. Physiological hurdles, limited carrying capacity, enhanced permeability and retention effect (EPR), nanoparticle variability, and regulatory and manufacturing concerns are among the challenges of employing nanoparticles for cancer therapy [**45**].

Due to the traditional side effects of chemo- and radiation therapy, silver nanoparticles have been shown to have a significant effect in fighting cancer in numerous studies. Furthermore, the development of safer, biocompatible, and effective cancer or anti-angiogenic agents containing AgNPs will increase the importance of AgNPs role in cancer prevention. On the other hand, the low toxicity of AgNPs on human health, dealing with biocompatibility of AgNPs and their interaction with cells and tissues, and reducing side effects [**46**].

CONCLUSION

Biopolymers are large molecules that are very interesting for modern applications. Polysaccharides have thus been identified and used in a variety of biomedical and biotechnological applications, including diagnosis, bioactive therapy, regulated drug delivery, gene therapy, cell encapsulation, tissue engineering, and medical devices. Nanoparticles are suitable for biomedical applications because they are biocompatible, biodegradable, have low cytotoxicity, and have a large number of surface functional groups that can be used for chemical modification. It's the first research to use a microwave-assisted extraction technique to extract a raw polysaccharide and synthesize polysaccharide coated silver nanoparticles from the *Ziziphus spina-Christi* plant. The raw polysaccharide and its AgNPs were available, and the analysis and characterization methods were accepted. The anticancer activity results showed that AgNPs was more powerful than raw polysaccharide toward hepg2 cancer cells. This discovery will pique interest in *Ziziphus spina-Christi* polysaccharide coated silver nanoparticles for potential biomedical applications.

ACKNOWLEDGMENT

This study project is funded by the Ministry of Higher Education and Scientific Research, the University of Basrah, the College of Education for Pure Sciences, and the Chemistry Department in Iraq as part of the master's degree requirements. The authors would like to thank Prof. Dr. Ali Abdullateef for his assistance with the MTT assay. The authors would like to express their gratitude to the Central Laboratory at the University of Tehran in Iran for their assistance with nanoparticle characterization and flow cytometry analysis.

DECLARATIONS OF INTEREST

The authors are declare there is no conflict of interest

REFERENCES

1. Al Shawi, A., Rasul, A., Khan, M., Iqbal, F., Tonghui, M. Eupatilin: A flavonoid compound isolated from the artemisia plant, induces apoptosis and G2/M phase cell cycle arrest in human melanoma A375 cells. African Journal of Pharmacy and Pharmacology 2011;5(5):582-588. DOI: 10.5897/AJPP11.079.
2. Mossa GD, Al-Shawi AA. Induction of apoptosis through S-phase in human breast cancer MDA-MB231 cells by ethanolic extract of dodonaea viscose L.-an Iraqi medicine plant. Journal of Basrah Researches (Sciences) 2015;41(1).
3. Cao B, Wei X-C, Xu X-R, Zhang H-Z, Luo C-H, Feng B, et al. Seeing the Unseen of the Combination of Two Natural Resins, Frankincense and Myrrh: Changes in Chemical Constituents and Pharmacological Activities. Molecules. 2019;24(17):3076.
4. Knez Hrnčič M, Ivanovski M, Cör D, Knez Ž. Chia Seeds (Salvia hispanica L.): An Overview-Phytochemical Profile, Isolation Methods, and Application. Molecules. 2019;25(1):11.
5. Hassan M, Bai j, Dou D-Q. Biopolymers; Definition, Classification and Applications. Egyptian Journal of Chemistry. 2019;0(0):0-.
6. Wróblewska-Krepsztul J, Rydzkowski T, Michalska-Pożoga I, Thakur VK. Biopolymers for Biomedical and Pharmaceutical Applications: Recent Advances and Overview of Alginate Electrospinning. Nanomaterials (Basel). 2019;9(3):404.
7. Liu D, Nikoo M, Boran G, Zhou P, Regenstein JM. Collagen and Gelatin. Annual Review of Food Science and Technology. 2015;6(1):527-57.
8. Chen L, Ge M-D, Zhu Y-J, Song Y, Cheung PCK, Zhang B-B, et al. Structure, bioactivity and applications of natural hyperbranched polysaccharides. Carbohydrate Polymers. 2019;223:115076.
9. Schepetkin IA, Quinn MT. Botanical polysaccharides: Macrophage immunomodulation and therapeutic potential. International Immunopharmacology. 2006;6(3):317-33.
10. Xie J-H, Jin M-L, Morris GA, Zha X-Q, Chen H-Q, Yi Y, et al. Advances on Bioactive Polysaccharides from Medicinal Plants. Critical Reviews in Food Science and Nutrition.

2015;56(sup1):S60-S84.
11. Yu W, Ren Z, Zhang X, Xing S, Tao S, Liu C, et al. Structural Characterization of Polysaccharides from Dendrobium officinale and Their Effects on Apoptosis of HeLa Cell Line. Molecules. 2018;23(10):2484.
12. Jiao R, Liu Y, Gao H, Xiao J, So KF. The Anti-Oxidant and Antitumor Properties of Plant Polysaccharides. The American Journal of Chinese Medicine. 2016;44(03):463-88.
13. Deng QF, Zhou X, Chen HG. Advance in study on hepatoprotective effects and its mechanism of polysaccharides. Zhongguo Zhong Yao Za Zhi. 2016;41(16):2958-2967. Chinese. doi: 10.4268/cjcmm2 01 61603.
14. El Maaiden E, El Kharrassi Y, Qarah NAS, Essamadi AK, Moustaid K, Nasser B. Genus Ziziphus: A comprehensive review on ethnopharmacological, phytochemical and pharmacological properties. Journal of Ethnopharmacology. 2020;259:112950.
15. Zait Y, Shtein I, Schwartz A. Long-term acclimation to drought, salinity and temperature in the thermophilic tree Ziziphus spina-christi: revealing different tradeoffs between mesophyll and stomatal conductance. Tree Physiology. 2018;39(5):701-16.
16. Almeer RS, Albasher G, Alotibi F, Alarifi S, Ali D, Alkahtani S. Ziziphus spina-christi Leaf Extract Suppressed Mercury Chloride-Induced Nephrotoxicity via Nrf2-Antioxidant Pathway Activation and Inhibition of Inflammatory and Apoptotic Signaling. Oxid Med Cell Longev. 2019;2019:5634685-.
17. Klębowski B, Depciuch J, Parlińska-Wojtan M, Baran J. Applications of Noble Metal-Based Nanoparticles in Medicine. Int J Mol Sci. 2018;19(12):4031.
18. McNamara K, Tofail SAM. Nanoparticles in biomedical applications. Advances in Physics: X. 2016;2(1):54-88.
19. Davatgaran Taghipour, Y., Kharrazi, S., Amini, S. Antibody Conjugated Gold Nanoparticles for Detection of Small Amounts of Antigen Based on Surface Plasmon Resonance (SPR) Spectra. *Nanomedicine Research Journal*, 2018; 3(2): 102-108. doi: 10.22034/nmrj.2018.02.007.
20. Amini SM. Preparation of antimicrobial metallic nanoparticles with bioactive compounds. Materials Science and Engineering: C. 2019;103:109809.
21. Zhang L, Gu FX, Chan JM, Wang AZ, Langer RS, Farokhzad OC. Nanoparticles in Medicine: Therapeutic Applications and Developments. Clinical Pharmacology & Therapeutics. 2007;83(5):761-9.
22. Rozman NAS, Tong WY, Leong CR, Tan WN, Hasanolbasori MA, Abdullah SZ. Potential Antimicrobial Applications of Chitosan Nanoparticles (ChNP). Journal of Microbiology and Biotechnology. 2019;29(7):1009-13.
23. Maity GN, Maity P, Choudhuri I, Sahoo GC, Maity N, Ghosh K, et al. Green synthesis, characterization, antimicrobial and cytotoxic effect of silver nanoparticles using arabinoxylan isolated from Kalmegh. International Journal of Biological Macromolecules. 2020;162:1025-34.
24. Yuan H, Li X, Tang J, Zhou M, Liu F. Local application of doxorubicin- loaded Iron oxid nanoparticles and the vascular disrupting agent via the hepatic artery: chemoembolization-photothermal ablation treatment of hepatocellular carcinoma in rats. Cancer Imaging. 2019;19(1):71-.
25. Jędrzak A, Grześkowiak BF, Golba K, Coy E, Synoradzki K, Jurga S, et al. Magnetite Nanoparticles and Spheres for Chemo- and Photothermal Therapy of Hepatocellular Carcinoma in vitro. Int J Nanomedicine. 2020;15:7923-36.
26. Xu J, Hou H, Hu J, Liu B. Optimized microwave extraction, characterization and antioxidant capacity of biological polysaccharides from Eucommia ulmoides Oliver leaf. Sci Rep. 2018;8(1):6561-.
27. Jain VM, Karibasappa GN, Dodamani AS, Mali GV. Estimating the carbohydrate content of various forms of tobacco by phenol-sulfuric acid method. J Educ Health Promot. 2017;6:90-.
28. TY Al-Abdullah, Z., Al-Shawi, A., Aboud, M., Al abdul aziz, B, QM Al-Furaiji, H., Luaibi, I. Synthesis and Analytical Characterization of Gold Nanoparticles using Microwave-Assisted Extraction System and Study their Application in Degradation. *Journal of Nanostructures*, 2020; 10(4): 682-690. doi: 10.22052/JNS.2020.04.001.
29. Khodaei, M. Characterization of Al2O3 in Fe3Al-30 vol.% Al2O3 nanocomposite powder synthesized by mechanochemical process. *Journal of Nanostructures*, 2020; 10(3): 456-462. doi: 10.22052/JNS.2020.03.003
30. Tolouietabar, H., Hatamnia, A., Sahraei, R., Soheyli, E. Biologically Green Synthesis of High-quality Silver Nanoparticles Using Scrophularia striata Boiss Plant Extract and Verifying Their Antibacterial Activities. *Journal of Nanostructures*, 2020; 10(1): 44-51. doi: 10.22052/JNS.2020.01.006
31. Mohammed MK, Al-Shuhaib Z, Al-Shawi AAA. Synthesis, characterization and cytotoxicity appraisal of original 1, 2, 3-Triazole derivatives, against breast cancer cell lines (MDA-MB-231). Mediterranean Journal of Chemistry. 2019;9(4):305-10.
32. Al-Shawi AAA, Hameed MF, Hussein KA, Neamah HF, Luaibi IN. Gas Chromatography-Mass Spectrometry Analysis of Bioactive Compounds of Iraqi Truffle Terfezia claveryi (Ascomycetes), Synthesis of Silver Nanoparticles, and Appraisal of Its Biological Activities. International Journal of Medicinal Mushrooms. 2021;23(3):79-89.
33. Khan M, Yu B, Rasul A, Al Shawi A, Yi F, Yang H, et al. Jaceosidin Induces Apoptosis in U87 Glioblastoma Cells through G2/M Phase Arrest. Evid Based Complement Alternat Med. 2012;2012:703034-.
34. Al-Shawi AAA, Hameed MF, Ali NH, Hussein KA. Investigations of Phytoconstituents, Antioxidant and Anti-Liver Cancer Activities of Saueda monoica Forssk Extracted by Microwave-Assisted Extraction. Asian Pac J Cancer Prev. 2020;21(8):2349-55.
35. Akhtar I, Javad S, Yousaf Z, Iqbal S, Jabeen K. Review: Microwave assisted extraction of phytochemicals an efficient and modern approach for botanicals and pharmaceuticals. Pak J Pharm Sci. 2019;32(1):223-230. PMID: 30772814.
36. Hameed M, Al-Shawi A. Phytochemical Analysis and Anticancer Evaluation of Iraqi Herb Chenopodium Murale Extracted by Microwave-assisted Extraction. International Medical Journal 2020; 25 (01):313-320.
37. Zhang Z-P, Shen C-C, Gao F-L, Wei H, Ren D-F, Lu J. Isolation, Purification and Structural Characterization of Two Novel Water-Soluble Polysaccharides from Anredera

cordifolia. Molecules. 2017;22(8):1276.
38. Liu Z, Gao T, Yang Y, Meng F, Zhan F, Jiang Q, et al. Anti-Cancer Activity of Porphyran and Carrageenan from Red Seaweeds. Molecules. 2019;24(23):4286.
39. Zhang Y, Jiang Y, Zhang M, Zhang L. Ganoderma sinense polysaccharide: An adjunctive drug used for cancer treatment. Progress in Molecular Biology and Translational Science: Elsevier; 2019. p. 165-77.
40. Sohretoglu D, Huang S. Ganoderma lucidum Polysaccharides as An Anti-cancer Agent. Anticancer Agents Med Chem. 2018;18(5):667-74.
41. Zhang Y, Cui Z, Mei H, Xu J, Zhou T, Cheng F, et al. Angelica sinensis polysaccharide nanoparticles as a targeted drug delivery system for enhanced therapy of liver cancer. Carbohydrate Polymers. 2019;219:143-54.
42. Akbari A, Majd HM, Rahnama R, Heshmati J, Morvaridzadeh M, Agah S, et al. Cross-talk between oxidative stress signaling and microRNA regulatory systems in carcinogenesis: Focused on gastrointestinal cancers. Biomedicine & Pharmacotherapy. 2020;131:110729.
43. Mortezaee K, Najafi M, Samadian H, Barabadi H, Azarnezhad A, Ahmadi A. Redox interactions and genotoxicity of metal-based nanoparticles: A comprehensive review. Chemico-Biological Interactions. 2019;312:108814.
44. Amini, S., Pirhajati Mahabadi, V. Selenium nanoparticles role in organ systems functionality and disorder. *Nanomedicine Research Journal*, 2018; 3(3): 117-124. doi: 10.22034/nmrj .2018.03.001
45. Amiri S, Yousefi-Ahmadipour A, Hosseini M-J, Haj-Mirzaian A, Momeny M, Hosseini-Chegeni H, et al. Maternal exposure to silver nanoparticles are associated with behavioral abnormalities in adulthood: Role of mitochondria and innate immunity in developmental toxicity. NeuroToxicology. 2018;66:66-77.